Measurement of $J/\psi \to \Xi(1530)^- \bar{\Xi}^+$ and evidence for the radiative decay $\Xi(1530)^- \to \gamma\Xi^-$

M. Ablikim,[1] M. N. Achasov,[10,d] P. Adlarson,[59] S. Ahmed,[15] M. Albrecht,[4] M. Alekseev,[58a,58c] A. Amoroso,[58a,58c] F. F. An,[1] Q. An,[55,43] Y. Bai,[42] O. Bakina,[27] R. Baldini Ferroli,[23a] I. Balossino,[24a] Y. Ban,[35] K. Begzsuren,[25] J. V. Bennett,[5] N. Berger,[26] M. Bertani,[23a] D. Bettoni,[24a] F. Bianchi,[58a,58c] J. Biernat,[59] J. Bloms,[52] I. Boyko,[27] R. A. Briere,[5] H. Cai,[60] X. Cai,[1,43] A. Calcaterra,[23a] G. F. Cao,[1,47] N. Cao,[1,47] S. A. Cetin,[46b] J. Chai,[58c] J. F. Chang,[1,43] W. L. Chang,[1,47] G. Chelkov,[27,b,c] D. Y. Chen,[6] G. Chen,[1] H. S. Chen,[1,47] J. C. Chen,[1] M. L. Chen,[1,43] S. J. Chen,[33] Y. B. Chen,[1,43] W. Cheng,[58c] G. Cibinetto,[24a] F. Cossio,[58c] X. F. Cui,[34] H. L. Dai,[1,43] J. P. Dai,[38,h] X. C. Dai,[1,47] A. Dbeyssi,[15] D. Dedovich,[27] Z. Y. Deng,[1] A. Denig,[26] I. Denysenko,[27] M. Destefanis,[58a,58c] F. De Mori,[58a,58c] Y. Ding,[31] C. Dong,[34] J. Dong,[1,43] L. Y. Dong,[1,47] M. Y. Dong,[1,43,47] Z. L. Dou,[33] S. X. Du,[63] J. Z. Fan,[45] J. Fang,[1,43] S. S. Fang,[1,47] Y. Fang,[1] R. Farinelli,[24a,24b] L. Fava,[58b,58c] F. Feldbauer,[4] G. Felici,[23a] C. Q. Feng,[55,43] M. Fritsch,[4] C. D. Fu,[1] Y. Fu,[1] Q. Gao,[1] X. L. Gao,[55,43] Y. Gao,[45] Y. Gao,[56] Y. G. Gao,[6] Z. Gao,[55,43] B. Garillon,[26] I. Garzia,[24a] E. M. Gersabeck,[50] A. Gilman,[51] K. Goetzen,[11] L. Gong,[34] W. X. Gong,[1,43] W. Gradl,[26] M. Greco,[58a,58c] L. M. Gu,[33] M. H. Gu,[1,43] S. Gu,[2] Y. T. Gu,[13] A. Q. Guo,[22] L. B. Guo,[32] R. P. Guo,[36] Y. P. Guo,[26] A. Guskov,[27] S. Han,[60] X. Q. Hao,[16] F. A. Harris,[48] K. L. He,[1,47] F. H. Heinsius,[4] T. Held,[4] Y. K. Heng,[1,43,47] M. Himmelreich,[11,g] Y. R. Hou,[47] Z. L. Hou,[1] H. M. Hu,[1,47] J. F. Hu,[38,h] T. Hu,[1,43,47] Y. Hu,[1] G. S. Huang,[55,43] J. S. Huang,[16] X. T. Huang,[37] X. Z. Huang,[33] N. Huesken,[52] T. Hussain,[57] W. Ikegami Andersson,[59] W. Imoehl,[22] M. Irshad,[55,43] Q. Ji,[1] Q. P. Ji,[16,*] X. B. Ji,[1,47] X. L. Ji,[1,43] H. L. Jiang,[37] X. S. Jiang,[1,43,47] X. Y. Jiang,[34] J. B. Jiao,[37] Z. Jiao,[18] D. P. Jin,[1,43,47] S. Jin,[33] Y. Jin,[49] T. Johansson,[59] N. Kalantar-Nayestanaki,[29] X. S. Kang,[31] R. Kappert,[29] M. Kavatsyuk,[29] B. C. Ke,[1] I. K. Keshk,[4] A. Khoukaz,[52] P. Kiese,[26] R. Kiuchi,[1] R. Kliemt,[11] L. Koch,[28] O. B. Kolcu,[46b,f] B. Kopf,[4] M. Kuemmel,[4] M. Kuessner,[4] A. Kupsc,[59] M. Kurth,[1] M. G. Kurth,[1,47] W. Kühn,[28] J. S. Lange,[28] P. Larin,[15] L. Lavezzi,[58c] H. Leithoff,[26] T. Lenz,[26] C. Li,[59] Cheng Li,[55,43] D. M. Li,[63] F. Li,[1,43] F. Y. Li,[35] G. Li,[1] H. B. Li,[1,47] H. J. Li,[9,j] J. C. Li,[1] J. W. Li,[41] Ke Li,[1] L. K. Li,[1] Lei Li,[3] P. L. Li,[55,43] P. R. Li,[30] Q. Y. Li,[37] W. D. Li,[1,47] W. G. Li,[1] X. H. Li,[55,43] X. L. Li,[37] X. N. Li,[1,43] Z. B. Li,[44] Z. Y. Li,[44] H. Liang,[55,43] H. Liang,[1,47] Y. F. Liang,[40] Y. T. Liang,[28] G. R. Liao,[12] L. Z. Liao,[1,47] J. Libby,[21] C. X. Lin,[44] D. X. Lin,[15] Y. J. Lin,[13] B. Liu,[38,h] B. J. Liu,[1] C. X. Liu,[1] D. Liu,[55,43] D. Y. Liu,[38,h] F. H. Liu,[39] Fang Liu,[1] Feng Liu,[6] H. B. Liu,[13] H. M. Liu,[1,47] Huanhuan Liu,[1] Huihui Liu,[17] J. B. Liu,[55,43] J. Y. Liu,[1,47] K. Y. Liu,[31] Ke Liu,[6] L. Y. Liu,[13] Q. Liu,[47] S. B. Liu,[55,43] T. Liu,[1,47] X. Liu,[30] X. Y. Liu,[1,47] Y. B. Liu,[34] Z. A. Liu,[1,43,47] Zhiqing Liu,[37] Y. F. Long,[35] X. C. Lou,[1,43,47] H. J. Lu,[18] J. D. Lu,[1,47] J. G. Lu,[1,43] Y. Lu,[1] Y. P. Lu,[1,43] C. L. Luo,[32] M. X. Luo,[62] P. W. Luo,[44] T. Luo,[9,j] X. L. Luo,[1,43] S. Lusso,[58c] X. R. Lyu,[47] F. C. Ma,[31] H. L. Ma,[1] L. L. Ma,[37] M. M. Ma,[1,47] Q. M. Ma,[1] X. N. Ma,[34] X. X. Ma,[1,47] X. Y. Ma,[1,43] Y. M. Ma,[37] F. E. Maas,[15] M. Maggiora,[58a,58c] S. Maldaner,[26] S. Malde,[53] Q. A. Malik,[57] A. Mangoni,[23b] Y. J. Mao,[35] Z. P. Mao,[1] S. Marcello,[58a,58c] Z. X. Meng,[49] J. G. Messchendorp,[29] G. Mezzadri,[24a] J. Min,[1,43] T. J. Min,[33] R. E. Mitchell,[22] X. H. Mo,[1,43,47] Y. J. Mo,[6] C. Morales Morales,[15] N. Yu. Muchnoi,[10,d] H. Muramatsu,[51] A. Mustafa,[4] S. Nakhoul,[11,g] Y. Nefedov,[27] F. Nerling,[11,g] I. B. Nikolaev,[10,d] Z. Ning,[1,43] S. Nisar,[8,k] S. L. Niu,[1,43] S. L. Olsen,[47] Q. Ouyang,[1,43,47] S. Pacetti,[23b] Y. Pan,[55,43] M. Papenbrock,[59] P. Patteri,[23a] M. Pelizaeus,[4] H. P. Peng,[55,43] K. Peters,[11,g] J. Pettersson,[59] J. L. Ping,[32] R. G. Ping,[1,47] A. Pitka,[4] R. Poling,[51] V. Prasad,[55,43] H. R. Qi,[45,†] M. Qi,[33] T. Y. Qi,[2] S. Qian,[1,43] C. F. Qiao,[47] N. Qin,[60] X. P. Qin,[13] X. S. Qin,[4] Z. H. Qin,[1,43] J. F. Qiu,[1] S. Q. Qu,[34] K. H. Rashid,[57,i] K. Ravindran,[21] C. F. Redmer,[26] M. Richter,[4] A. Rivetti,[58c] V. Rodin,[29] M. Rolo,[58c] G. Rong,[1,47] Ch. Rosner,[15] M. Rump,[52] A. Sarantsev,[27,e] Y. Schelhaas,[26] K. Schoenning,[59] W. Shan,[19] X. Y. Shan,[55,43] M. Shao,[55,43] C. P. Shen,[2] P. X. Shen,[34] X. Y. Shen,[1,47] H. Y. Sheng,[1] X. Shi,[1,43] X. D. Shi,[55,43] J. J. Song,[37] Q. Q. Song,[55,43] X. Y. Song,[1] S. Sosio,[58a,58c] C. Sowa,[4] S. Spataro,[58a,58c] F. F. Sui,[37] G. X. Sun,[1] J. F. Sun,[16] L. Sun,[60] S. S. Sun,[1,47] X. H. Sun,[1] Y. J. Sun,[55,43] Y. K. Sun,[55,43] Y. Z. Sun,[1] Z. J. Sun,[1,43] Z. T. Sun,[1] Y. T. Tan,[55,43] C. J. Tang,[40] G. Y. Tang,[1] X. Tang,[1] V. Thoren,[59] B. Tsednee,[25] I. Uman,[46d] B. Wang,[1] B. L. Wang,[47] C. W. Wang,[33] D. Y. Wang,[35] K. Wang,[1,43] L. L. Wang,[1] L. S. Wang,[1] M. Wang,[37] M. Z. Wang,[35] Meng Wang,[1,47] P. L. Wang,[1] R. M. Wang,[61] W. P. Wang,[55,43] X. Wang,[35] X. F. Wang,[1] X. L. Wang,[9,j] Y. Wang,[55,43] Y. Wang,[44] Y. F. Wang,[1,43,47] Z. Wang,[1,43] Z. G. Wang,[1,43] Z. Y. Wang,[1] Zongyuan Wang,[1,47] T. Weber,[4] D. H. Wei,[12] P. Weidenkaff,[26] H. W. Wen,[32] S. P. Wen,[1] U. Wiedner,[4] G. Wilkinson,[53] M. Wolke,[59] L. H. Wu,[1] L. J. Wu,[1,47] Z. Wu,[1,43] L. Xia,[55,43] Y. Xia,[20] S. Y. Xiao,[1] Y. J. Xiao,[1,47] Z. J. Xiao,[32] Y. G. Xie,[1,43] Y. H. Xie,[6] T. Y. Xing,[1,47] X. A. Xiong,[1,47] Q. L. Xiu,[1,43] G. F. Xu,[1] J. J. Xu,[33] L. Xu,[1] Q. J. Xu,[14] W. Xu,[1,47] X. P. Xu,[41] F. Yan,[56] L. Yan,[58a,58c] W. B. Yan,[55,43] W. C. Yan,[2] Y. H. Yan,[20] H. J. Yang,[38,h] H. X. Yang,[1] L. Yang,[60] R. X. Yang,[55,43] S. L. Yang,[1,47] Y. H. Yang,[33] Y. X. Yang,[12] Yifan Yang,[1,47] Z. Q. Yang,[20] M. Ye,[1,43] M. H. Ye,[7] J. H. Yin,[1] Z. Y. You,[44] B. X. Yu,[1,43,47] C. X. Yu,[34] J. S. Yu,[20] T. Yu,[56] C. Z. Yuan,[1,47] X. Q. Yuan,[35] Y. Yuan,[1] A. Yuncu,[46b,a] A. A. Zafar,[57] Y. Zeng,[20] B. X. Zhang,[1] B. Y. Zhang,[1,43] C. C. Zhang,[1] D. H. Zhang,[1] H. H. Zhang,[44] H. Y. Zhang,[1,43] J. Zhang,[1,47] J. L. Zhang,[61] J. Q. Zhang,[4] J. W. Zhang,[1,43,47] J. Y. Zhang,[1] J. Z. Zhang,[1,47] K. Zhang,[1,47] L. M. Zhang,[45] S. F. Zhang,[33] T. J. Zhang,[38,h] X. Y. Zhang,[37] Y. Zhang,[55,43] Y. H. Zhang,[1,43] Y. T. Zhang,[55,43] Yang Zhang,[1]

2470-0010/2020/101(1)/012004(11) Published by the American Physical Society

Yao Zhang,[1] Yi Zhang,[9,j] Yu Zhang,[47] Z. H. Zhang,[6] Z. P. Zhang,[55] Z. Y. Zhang,[60] G. Zhao,[1] J. W. Zhao,[1,43] J. Y. Zhao,[1,47] J. Z. Zhao,[1,43] Lei Zhao,[55,43] Ling Zhao,[1] M. G. Zhao,[34] Q. Zhao,[1] S. J. Zhao,[63] T. C. Zhao,[1] Y. B. Zhao,[1,43] Z. G. Zhao,[55,43] A. Zhemchugov,[27,b] B. Zheng,[56] J. P. Zheng,[1,43] Y. Zheng,[35] Y. H. Zheng,[47] B. Zhong,[32] L. Zhou,[1,43] L. P. Zhou,[1,47] Q. Zhou,[1,47] X. Zhou,[60] X. K. Zhou,[47] X. R. Zhou,[55,43] Xiaoyu Zhou,[20] Xu Zhou,[20] A. N. Zhu,[1,47] J. Zhu,[34] J. Zhu,[44] K. Zhu,[1] K. J. Zhu,[1,43,47] S. H. Zhu,[54] W. J. Zhu,[34] X. L. Zhu,[45] Y. C. Zhu,[55,43] Y. S. Zhu,[1,47] Z. A. Zhu,[1,47] J. Zhuang,[1,43] B. S. Zou,[1] and J. H. Zou[1]

(BESIII Collaboration)

[1]*Institute of High Energy Physics, Beijing 100049, People's Republic of China*
[2]*Beihang University, Beijing 100191, People's Republic of China*
[3]*Beijing Institute of Petrochemical Technology, Beijing 102617, People's Republic of China*
[4]*Bochum Ruhr-University, D-44780 Bochum, Germany*
[5]*Carnegie Mellon University, Pittsburgh, Pennsylvania 15213, USA*
[6]*Central China Normal University, Wuhan 430079, People's Republic of China*
[7]*China Center of Advanced Science and Technology, Beijing 100190, People's Republic of China*
[8]*COMSATS University Islamabad, Lahore Campus, Defence Road, Off Raiwind Road, 54000 Lahore, Pakistan*
[9]*Fudan University, Shanghai 200443, People's Republic of China*
[10]*G.I. Budker Institute of Nuclear Physics SB RAS (BINP), Novosibirsk 630090, Russia*
[11]*GSI Helmholtzcentre for Heavy Ion Research GmbH, D-64291 Darmstadt, Germany*
[12]*Guangxi Normal University, Guilin 541004, People's Republic of China*
[13]*Guangxi University, Nanning 530004, People's Republic of China*
[14]*Hangzhou Normal University, Hangzhou 310036, People's Republic of China*
[15]*Helmholtz Institute Mainz, Johann-Joachim-Becher-Weg 45, D-55099 Mainz, Germany*
[16]*Henan Normal University, Xinxiang 453007, People's Republic of China*
[17]*Henan University of Science and Technology, Luoyang 471003, People's Republic of China*
[18]*Huangshan College, Huangshan 245000, People's Republic of China*
[19]*Hunan Normal University, Changsha 410081, People's Republic of China*
[20]*Hunan University, Changsha 410082, People's Republic of China*
[21]*Indian Institute of Technology Madras, Chennai 600036, India*
[22]*Indiana University, Bloomington, Indiana 47405, USA*
[23a]*INFN Laboratori Nazionali di Frascati, I-00044, Frascati, Italy*
[23b]*INFN and University of Perugia, I-06100, Perugia, Italy*
[24a]*INFN Sezione di Ferrara, I-44122, Ferrara, Italy*
[24b]*University of Ferrara, I-44122, Ferrara, Italy*
[25]*Institute of Physics and Technology, Peace Ave. 54B, Ulaanbaatar 13330, Mongolia*
[26]*Johannes Gutenberg University of Mainz, Johann-Joachim-Becher-Weg 45, D-55099 Mainz, Germany*
[27]*Joint Institute for Nuclear Research, 141980 Dubna, Moscow region, Russia*
[28]*Justus-Liebig-Universitaet Giessen, II. Physikalisches Institut, Heinrich-Buff-Ring 16, D-35392 Giessen, Germany*
[29]*KVI-CART, University of Groningen, NL-9747 AA Groningen, Netherlands*
[30]*Lanzhou University, Lanzhou 730000, People's Republic of China*
[31]*Liaoning University, Shenyang 110036, People's Republic of China*
[32]*Nanjing Normal University, Nanjing 210023, People's Republic of China*
[33]*Nanjing University, Nanjing 210093, People's Republic of China*
[34]*Nankai University, Tianjin 300071, People's Republic of China*
[35]*Peking University, Beijing 100871, People's Republic of China*
[36]*Shandong Normal University, Jinan 250014, People's Republic of China*
[37]*Shandong University, Jinan 250100, People's Republic of China*
[38]*Shanghai Jiao Tong University, Shanghai 200240, People's Republic of China*
[39]*Shanxi University, Taiyuan 030006, People's Republic of China*
[40]*Sichuan University, Chengdu 610064, People's Republic of China*
[41]*Soochow University, Suzhou 215006, People's Republic of China*
[42]*Southeast University, Nanjing 211100, People's Republic of China*
[43]*State Key Laboratory of Particle Detection and Electronics, Beijing 100049, Hefei 230026, People's Republic of China*
[44]*Sun Yat-Sen University, Guangzhou 510275, People's Republic of China*
[45]*Tsinghua University, Beijing 100084, People's Republic of China*

[46a]Ankara University, 06100 Tandogan, Ankara, Turkey
[46b]Istanbul Bilgi University, 34060 Eyup, Istanbul, Turkey
[46c]Uludag University, 16059 Bursa, Turkey
[46d]Near East University, Nicosia, North Cyprus, Mersin 10, Turkey
[47]University of Chinese Academy of Sciences, Beijing 100049, People's Republic of China
[48]University of Hawaii, Honolulu, Hawaii 96822, USA
[49]University of Jinan, Jinan 250022, People's Republic of China
[50]University of Manchester, Oxford Road, Manchester, M13 9PL, United Kingdom
[51]University of Minnesota, Minneapolis, Minnesota 55455, USA
[52]University of Muenster, Wilhelm-Klemm-Str. 9, 48149 Muenster, Germany
[53]University of Oxford, Keble Rd, Oxford, United Kingdom OX13RH
[54]University of Science and Technology Liaoning, Anshan 114051, People's Republic of China
[55]University of Science and Technology of China, Hefei 230026, People's Republic of China
[56]University of South China, Hengyang 421001, People's Republic of China
[57]University of the Punjab, Lahore-54590, Pakistan
[58a]University of Turin, I-10125, Turin, Italy
[58b]University of Eastern Piedmont, I-15121, Alessandria, Italy
[58c]INFN, I-10125, Turin, Italy
[59]Uppsala University, Box 516, SE-75120 Uppsala, Sweden
[60]Wuhan University, Wuhan 430072, People's Republic of China
[61]Xinyang Normal University, Xinyang 464000, People's Republic of China
[62]Zhejiang University, Hangzhou 310027, People's Republic of China
[63]Zhengzhou University, Zhengzhou 450001, People's Republic of China

(Received 18 November 2019; published 8 January 2020)

The SU(3)-flavor violating decay $J/\psi \to \Xi(1530)^-\bar{\Xi}^+ + \mathrm{c.c.}$ is studied using $(1310.6 \pm 7.0) \times 10^6$ J/ψ events collected with the BESIII detector at BEPCII, and the branching fraction is measured to be $\mathcal{B}(J/\psi \to \Xi(1530)^-\bar{\Xi}^+ + \mathrm{c.c.}) = (3.17 \pm 0.02_{\mathrm{stat}} \pm 0.08_{\mathrm{syst}}) \times 10^{-4}$. This result is consistent with previous measurements with an order of magnitude improved precision. The angular parameter for this decay is measured for the first time and is found to be $\alpha = -0.21 \pm 0.04_{\mathrm{stat}} \pm 0.06_{\mathrm{syst}}$. In addition, we report evidence for the radiative decay $\Xi(1530)^- \to \gamma\Xi^-$ with a significance of 3.9σ, including the systematic uncertainties. The 90% confidence level upper limit on the branching fraction is determined to be $\mathcal{B}(\Xi(1530)^- \to \gamma\Xi^-) \leq 3.7\%$.

DOI: 10.1103/PhysRevD.101.012004

[*]Corresponding author.
jiqingping@htu.edu.cn
[†]Corresponding author.
qihongrong@tsinghua.edu.cn
[a]Also at Bogazici University, 34342 Istanbul, Turkey.
[b]Also at the Moscow Institute of Physics and Technology, Moscow 141700, Russia.
[c]Also at the Functional Electronics Laboratory, Tomsk State University, Tomsk, 634050, Russia.
[d]Also at the Novosibirsk State University, Novosibirsk, 630090, Russia.
[e]Also at the NRC "Kurchatov Institute", PNPI, 188300, Gatchina, Russia.
[f]Also at Istanbul Arel University, 34295 Istanbul, Turkey.
[g]Also at Goethe University Frankfurt, 60323 Frankfurt am Main, Germany.
[h]Also at Key Laboratory for Particle Physics, Astrophysics and Cosmology, Ministry of Education; Shanghai Key Laboratory for Particle Physics and Cosmology; Institute of Nuclear and Particle Physics, Shanghai 200240, People's Republic of China.
[i]Also at Government College Women University, Sialkot - 51310. Punjab, Pakistan.
[j]Also at Key Laboratory of Nuclear Physics and Ion-beam Application (MOE) and Institute of Modern Physics, Fudan University, Shanghai 200443, People's Republic of China.
[k]Also at Harvard University, Department of Physics, Cambridge, Massachusetts, 02138, USA.

I. INTRODUCTION

The Ξ and $\Xi(1530)$ hyperons are regarded as SU(3) octet (orbital angular momentum within quarks $L = 0$ and spin-parity $J^P = \frac{1}{2}^+$) and decuplet ($L = 0$ and $J^P = \frac{3}{2}^+$) baryons, respectively [1–3]. In this context, the process $J/\psi \to \Xi(1530)^- \bar{\Xi}^+$ [4] should be suppressed by the SU (3)-flavor symmetry [1,2,5]. Nevertheless, a sizable branching fraction of $(5.9 \pm 1.5) \times 10^{-4}$ [6,7] for the decay $J/\psi \to \Xi(1530)^- \bar{\Xi}^+$ was measured based on $(8.6 \pm 1.3) \times 10^6$ J/ψ events by the DM2 Collaboration in 1982 and $(0.70 \pm 0.12) \times 10^{-5}$ for the decay $\psi(3686) \to \Xi(1530)^- \bar{\Xi}^+$ based on $(448.1 \pm 2.9) \times 10^6$ $\psi(3686)$ events by the BESIII Collaboration in 2019 [8]. For comparison, the SU(3)-flavor violating decay $J/\psi \to \Delta^+ \bar{p}$ has a branching fraction of less than 1×10^{-4} [7] at 90% confidence level (C.L.), while the SU(3)-allowed decays $J/\psi \to p\bar{p}$ and $J/\psi \to N(1535)^+ \bar{p}$ [1] have branching fractions of $(1-2) \times 10^{-3}$ [9]. Therefore, the branching fraction for $J/\psi \to \Xi(1530)^- \bar{\Xi}^+$ [7] is anomalously large when compared to that of $J/\psi \to \Xi^- \bar{\Xi}^+$, which is measured to be $(0.98 \pm 0.08) \times 10^{-3}$ [9]. An explanation for this anomaly is that a substantial $J^P = \frac{1}{2}^-$ component may hide underneath the $J^P = \frac{3}{2}^+$ peak while the branching fraction for $J/\psi \to \Xi(1530)^- \bar{\Xi}^+$ was obtained assuming a pure $\frac{3}{2}^+$ contribution around 1530 MeV/c^2 [1]. An isodoublet Ξ^* state with $J^P = \frac{1}{2}^-$ around 1520 MeV/c^2 [10], called $\Xi(1520)$, is predicted in the diquark cluster picture, which is an SU(3) pentaquark octet with a $[ds][su]\bar{u}$ component. Due to the small number of event in the analysis of $J/\psi \to \Xi(1530)^- \bar{\Xi}^+$ reported by DM2 [7], it is difficult to give a solid conclusion on whether a $\frac{1}{2}^-$ partial wave contributes to the $\Xi(1530)$ mass region.

BESIII collected $(1310.6 \pm 7.0) \times 10^6$ J/ψ events [11,12] in 2009 and 2012, a 2 orders of magnitude larger statistics than available to the DM2 experiment. A precision measurement with the BESIII experiment was therefore performed.

In 1981, Brodsky and Lepage [13] were the first to note the significance of angular distributions as a test of quantum chromodynamics. According to Ref. [13], the angular distribution of the J/ψ decay to a baryon-antibaryon ($B\bar{B}$) pair is defined by

$$\frac{dN}{d\cos\theta} \propto 1 + \alpha \cos^2\theta, \tag{1}$$

where θ is the polar angle between the baryon direction and the positron beam direction in the J/ψ rest frame, and α is a constant that parametrizes the angular distribution. The value of α has been predicted in many theoretical approaches for the SU(3)-allowed charmonium decays, such as electromagnetic contributions [14], quark mass effects [15,16], rescattering effects [17], etc. Considering electromagnetic contributions while ignoring quark mass effects in the SU(3)-allowed $J/\psi \to B\bar{B}$ decays, the parameter α is expressed [14] as

$$\alpha = \frac{m_{J/\psi}^2 - 4M_B^2}{m_{J/\psi}^2 + 4M_B^2},$$

where $m_{J/\psi}$ is the nominal J/ψ mass [9] and M_B refers to a baryon mass. Yet Carimalo [15] deemed that quark mass effects are more sensitive than electromagnetic contributions to the α value. He provided the formula [15],

$$\alpha = \frac{(1+u)^2 - u(1+6u)^2}{(1+u)^2 + u(1+6u)^2},$$

with $u = M_B^2/m_\psi^2$ (m_ψ denotes a charmonium resonance mass), which fits the experimental data better than when only considering electromagnetic effects. It is easy to see that $0 < \alpha < 1$ in the above-mentioned parametrizations. However, BESIII previously measured a negative α values for $J/\psi \to \Sigma^0 \bar{\Sigma}^0$ and $\Sigma(1385)\bar{\Sigma}(1385)$ [18,19]. Chen and Ping [17] investigated the rescattering effects of $B\bar{B}$ in heavy quarkonium decays. As a result, the resulting angular distribution parameter α can be negative. However, there are no theoretical predictions or experimental data available on the angular distributions for SU(3)-flavor violating J/ψ decays. Measurements of angular distributions of such decays have the potential to bring more insight into the SU(3)-flavor violating mechanism.

In addition, the electromagnetic transition of decuplet to octet hyperons is a very sensitive probe of their structures [3,20–22]. The partial width of the radiative transition $\Xi(1530)^- \to \gamma \Xi^-$ is estimated to be 3.1 keV when considering meson cloud effects with a relativistic quark model [3] in which the valence quark contributions for a baryon are supplemented by the pion or kaon cloud, and about 3 keV when considering octet-decuplet mixing with a nonrelativistic potential model [20]. Taking into account the total decay width of $\Xi(1530)^-$ of 9.9 MeV [9], the branching fraction of $\Xi(1530)^- \to \gamma \Xi^-$ is inferred to be about 3.0×10^{-4}. Experimentally, only an upper limit for $\mathcal{B}(\Xi(1530)^- \to \gamma \Xi^-) < 4\%$ is reported at the 90% C.L. in 1975 [23].

In this analysis, based on $(1310.6 \pm 7.0) \times 10^6$ J/ψ events [12] collected with the BEijing Spectrometer III (BESIII) at the Beijing Electron-Positron Collider (BEPCII), we measure the branching fraction of $J/\psi \to \Xi(1530)^- \bar{\Xi}^+$ with an improved precision and determine the angular distribution parameter for the first time. In addition, we also report evidence for the $\Xi(1530)^- \to \gamma \Xi^-$ decay with a 3.9σ significance based on the $J/\psi \to \Xi(1530)^- \bar{\Xi}^+$ process, and the corresponding 90% C.L. upper limit on the branching fraction is given.

II. BESIII DETECTOR AND MONTE CARLO SIMULATION

The BESIII detector operating at the BEPCII collider is described in detail in Ref. [24]. The detector is cylindrically symmetric and covers 93% of 4π solid angle. It consists of the following four subdetectors: a 43-layer main drift chamber (MDC), which is used to determine momenta of charged tracks with a resolution of 0.5% at 1 GeV/c in an axial magnetic field of 1 T with the 2009 data set and 0.9 T with the 2012 data set; a plastic scintillator time-of-flight system (TOF), with a time resolution of 80 ps (110 ps) in the barrel (end caps); an electromagnetic calorimeter (EMC) consisting of 6240 CsI(Tl) crystals, with relative photon energy resolution of 2.5% (5%) at 1 GeV in the barrel (end caps); and a muon counter consisting of 9 (8) layers of resistive plate chambers in the barrel (end caps), with a position resolution of 2 cm.

The response of the BESIII detector is modeled with Monte Carlo (MC) simulations using the software framework BOOST [25] based on GEANT4 [26,27], which includes the geometry and material description of the BESIII detectors, the detector response and digitization models, as well as a database that keeps track of the running conditions and the detector performance. MC samples are used to optimize the selection criteria, evaluate the signal efficiency, and estimate backgrounds. Two signal MC samples of 0.3 million events each have been generated with the J2BB3 model [28] for the $J/\psi \to \Xi(1530)^-\bar{\Xi}^+$ reaction. The first MC sample contains inclusive $\Xi(1530)^-$ decays and the second sample consists of exclusive $\Xi(1530)^- \to \gamma\Xi^-$ decay using the angular distribution constant α [see Eq. (1) of Ref. [28]] as measured in this analysis. Only the baryon decays $\bar{\Xi}^+ \to \bar{\Lambda}\pi^+$ and $\bar{\Lambda} \to \bar{p}\pi^+$ in the signal channels are simulated. An inclusive MC sample of 1.225×10^9 J/ψ events is used for the background studies. Here, the J/ψ resonance is produced by means of the KKMC event generator [29], in which the initial state radiation is included. The decays are simulated by EVTGEN [30] with the known branching fractions taken from the Particle Data Group (PDG) [9], while the remaining unmeasured decay modes are generated with LUNDCHARM [31].

III. DATA ANALYSIS

A. $J/\psi \to \Xi(1530)^-\bar{\Xi}^+$ with $\Xi(1530)^- \to$ anything

For the inclusive analysis of the $\Xi(1530)^-$ decay, a single tagged (ST) $\bar{\Xi}^+$ baryon candidate is reconstructed via $\bar{\Lambda}(\to \bar{p}\pi^+)\pi^+$, while the $\Xi(1530)^-$ candidate is treated as a missing particle. The presence of a $\Xi(1530)^-$ candidate is inferred using the mass recoiling against the $\bar{\Lambda}\pi^+$ system, $M^{\rm recoil}_{\bar{\Lambda}\pi^+} = \sqrt{(E - E_{\bar{\Lambda}\pi^+})^2 - (\boldsymbol{P}_{\bar{\Lambda}\pi^+})^2}$, where E is the center-of-mass (c.m.) energy and $(E_{\bar{\Lambda}\pi^+}, \boldsymbol{P}_{\bar{\Lambda}\pi^+})$ is the four momenta of the $\bar{\Lambda}\pi^+$ system in the e^+e^- rest frame. For signal candidate events, the distribution of $M^{\rm recoil}_{\bar{\Lambda}\pi^+}$ will form a peak around the nominal mass of the charged $\Xi(1530)^-$ resonance [9].

Charged tracks must be properly reconstructed in the MDC with $|\cos\theta| < 0.93$, where θ is the polar angle between the charged track and the positron beam direction. The combined information from the TOF and ionization loss (dE/dx) in the MDC is used to calculate particle identification confidence levels for each hadron (i) hypothesis ($i = p, \pi, K$). A charged track is identified as the ith particle type with the highest confidence level. Events with at least one antiproton (proton) and two positively (negatively) charged pions are selected for tagging the $\bar{\Xi}^+$ (Ξ^-) decay mode.

The $\bar{\Lambda}$ candidates are reconstructed with a vertex fit to all the identified $\bar{p}\pi^+$ combinations. A secondary vertex fit [32] is then employed to the $\bar{\Lambda}$ candidates, and events are kept if the decay length, i.e., the distance from the production vertex to the decay vertex, is greater than zero. If there remains more than one $\bar{p}\pi^+$ combination in the event, the one closest to the nominal $\bar{\Lambda}$ mass [9] is retained. A $\bar{\Lambda}$ signal is required to have a $\bar{p}\pi^+$ invariant mass within 5 MeV/c^2 from the nominal $\bar{\Lambda}$ mass [9]. The $\bar{\Xi}^+$ candidates are reconstructed via a secondary vertex fit by considering all combinations of the extra charged pions and the selected $\bar{\Lambda}$ candidate, requiring that the decay length of the reconstructed $\bar{\Xi}^+$ candidates are greater than zero. If several combinations remain, the one with the minimum $|M_{\bar{\Lambda}\pi^+} - m_{\bar{\Xi}^+}|$, where $M_{\bar{\Lambda}\pi^+}$ is the invariant mass of the $\bar{\Lambda}\pi^+$ system and $m_{\bar{\Xi}^+}$ is the nominal mass of the $\bar{\Xi}^+$ baryon [9], is selected. Additionally, the requirement $|M_{\bar{\Lambda}\pi^+} - m_{\bar{\Xi}^+}| \leq 8$ MeV/c^2 is applied to further suppress the backgrounds.

After applying the above selection criteria, a scatter plot of $M^{\rm recoil}_{\bar{\Lambda}\pi^+}$ versus $M^{\rm ST}_{\bar{\Lambda}\pi^+}$ is shown in Fig. 1 (left), where $M^{\rm ST}_{\bar{\Lambda}\pi^+}$ is the $\bar{\Lambda}\pi^+$ invariant mass in the ST mode, and significantly clustered events of the SU(3)-flavor violating $J/\psi \to \Xi(1530)^-\bar{\Xi}^+$ decay are observed in the data. Figure 1 (middle) illustrates the distribution of $M^{\rm ST}_{\bar{\Lambda}\pi^+}$. In both figures, the red solid and green long-dashed lines indicate the $\bar{\Xi}^+$ signal and sideband regions, respectively. The $\Xi(1530)^-$ signal in the $M^{\rm recoil}_{\bar{\Lambda}\pi^+}$ spectrum has a Breit-Winger shape, as shown in Fig. 1 (right).

The continuum data collected at the c.m. energy of 3.08 GeV, with an integrated luminosity of 30 pb^{-1} [11,12], are used to investigate the contribution from the quantum electrodynamics (QED) process $e^+e^- \to \Xi(1530)^-\bar{\Xi}^+$. By imposing the same event selection criteria as the J/ψ data, no events survived, meaning that the QED background is negligible. The contamination from the non-$\bar{\Xi}^+$ backgrounds is estimated with the $\bar{\Xi}^+$ mass sideband events, where the sideband regions are selected as

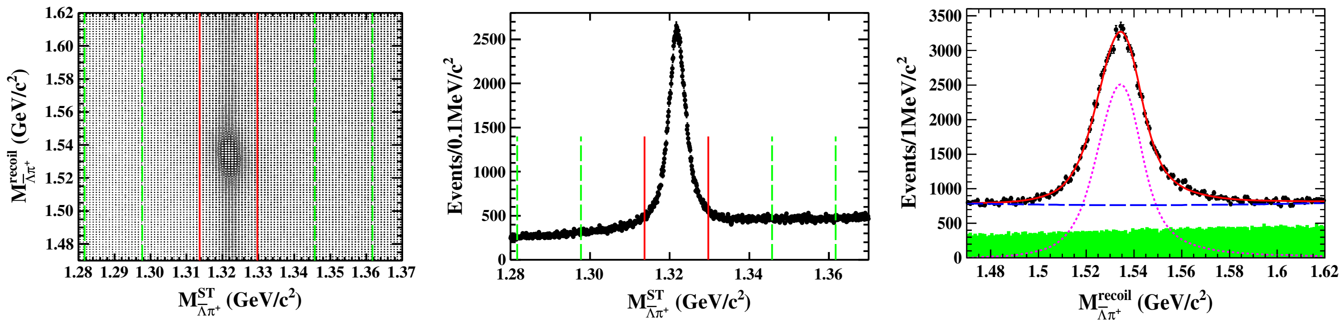

FIG. 1. Left: scatter plot of $M^{\mathrm{recoil}}_{\bar{\Lambda}\pi^+}$ versus $M^{\mathrm{ST}}_{\bar{\Lambda}\pi^+}$ from the data, where $M^{\mathrm{ST}}_{\bar{\Lambda}\pi^+}$ is the $\bar{\Lambda}\pi^+$ invariant mass in the ST mode. Middle: the $M^{\mathrm{ST}}_{\bar{\Lambda}\pi^+}$ distribution in the data. The red solid and green long-dashed lines indicate the $\bar{\Xi}^+$ signal and sideband regions, respectively. Right: fit to the experimental $M^{\mathrm{recoil}}_{\bar{\Lambda}\pi^+}$ distribution. The red solid line is the fit result, the pink dotted line denotes the signal component, the blue long-dashed line represents the fitted background component, and the green-shaded histogram represents the normalized $\bar{\Xi}^+$ mass sideband events from the data.

$M^{\mathrm{ST}}_{\bar{\Lambda}\pi^+} \in [1.2817, 1.2977] \cup [1.3457, 1.3617]$ GeV$/c^2$, as indicated by the green long-dashed lines in Fig. 1 (middle). No peaking background is found in the $\Xi(1530)^-$ signal region from the $\bar{\Xi}^+$ mass sideband events, as indicated by the green-shaded histogram in Fig. 1 (right). The remaining backgrounds, investigated by the inclusive MC sample, form a smooth distribution in the $M^{\mathrm{recoil}}_{\bar{\Lambda}\pi^+}$ spectrum in the region of 1.535 GeV$/c^2$, where the main contributions are from $J/\psi \to \Xi^-\bar{\Xi}^+\pi^0$ and $J/\psi \to \Xi^0\bar{\Xi}^+\pi^-$ events.

The signal yields of the $J/\psi \to \Xi(1530)^-\bar{\Xi}^+$ decay are extracted from an unbinned maximum likelihood fit to the $M^{\mathrm{recoil}}_{\bar{\Lambda}\pi^+}$ spectrum. The $\Xi(1530)^-$ signal is described by the simulated MC shape convolved with a Gaussian function, which accounts for the mass resolution difference between the data and MC simulation. The mean of the Gaussian function is fixed to zero while the standard deviation is a free parameter. The background contribution is described by a second-order Chebychev polynomial function. The fit of the $M^{\mathrm{recoil}}_{\bar{\Lambda}\pi^+}$ spectrum in data is shown in Fig. 1 (right), and the fitted signal yields are listed in Table I.

B. $J/\psi \to \Xi(1530)^-\bar{\Xi}^+$ with $\Xi(1530)^- \to \gamma\Xi^-$

The event selection criteria for the radiative decay $\Xi(1530)^- \to \gamma\Xi^-$ are based on the $\bar{\Xi}^+$ tagging mode.

TABLE I. Numerical results on the branching fraction measurement for $J/\psi \to \Xi(1530)^-\bar{\Xi}^+$. The uncertainties are statistical only.

$N^{\mathrm{obs}}_{\mathrm{ST}}$	70186 ± 544
$N_{J/\psi}$	1310.6×10^6
$\mathcal{B}(\bar{\Xi} \to \bar{\Lambda}\pi^+)$	99.89%
$\mathcal{B}(\bar{\Lambda} \to \bar{p}\pi^+)$	63.90%
$\epsilon^{\Xi^-}_{\mathrm{ST}}$ ($\epsilon^{\bar{\Xi}^+}_{\mathrm{ST}}$)	24.03% (25.57%)
f^- (f^+)	1.079 ± 0.011 (1.053 ± 0.011)
Branching fraction ($\times 10^{-4}$)	3.17 ± 0.02

Besides the tagged $\bar{\Xi}^+$ candidates described in Sec. III A, an extra Ξ^- baryon and a photon are selected to reconstruct the $\Xi(1530)^-$ candidate. Since all decay particles from $\Xi(1530)^-$ and $\bar{\Xi}^+$ are reconstructed from the $J/\psi \to \Xi(1530)^-\bar{\Xi}^+$ process, it is referred to as the double tag (DT) mode. The event selection of Ξ^- candidates is similar to those of tagged $\bar{\Xi}^+$ candidates in Sec. III A, except for the charge-conjugated final states. The Ξ^- candidate with the minimum $|M^{\mathrm{DT}}_{\Lambda\pi^-} - m_{\Xi^-}|$ is the only one retained, and then is requirement $|M^{\mathrm{DT}}_{\Lambda\pi^-} - m_{\Xi^-}| \leq 8$ MeV$/c^2$ applied. The Ξ^- mass window is shown by the red solid lines in Fig. 2 (left and middle), where $M^{\mathrm{DT}}_{\Lambda\pi^-}$ is the invariant mass of the $\Lambda\pi^-$ system in the DT mode, and m_{Ξ^-} is the nominal mass of the Ξ^- baryon [9].

Photons are reconstructed by clustering the EMC crystals' signals, and the energy deposited in the nearby TOF counter is included to improve the reconstruction efficiency and energy resolution [24]. A photon candidate is defined as a shower with an energy deposit of at least 25 MeV in the barrel region ($|\cos\theta < 0.8|$) or of at least 50 MeV in the end cap region ($|0.86 < \cos\theta| < 0.92$). Showers in the angular range between the barrel and the end caps are poorly reconstructed and therefore excluded. An additional requirement on the EMC timing of a photon candidate, $0 \leq t \leq 700$ ns, is employed to suppress electronic noise and energy deposits unrelated to the collision event, where time is measured relative to the event start time. All photons, which satisfy the above selection criteria are kept for further analysis.

A four-constraint (4C) kinematic fit is performed for events with γ, Ξ^-, and $\bar{\Xi}^+$ candidates by imposing overall energy-momentum conservation. For each event, the combination with the lowest $\chi^2_{4\mathrm{C}}$ is selected. To suppress background events different from the final states of the signal channel, we require $\chi^2_{4\mathrm{C}} < 5$, which is determined by maximizing the figure-of-merit $\mathrm{FOM} = S/\sqrt{S+B}$. Here, S is the expected number of signal events from the signal MC simulation and B is the number of background events

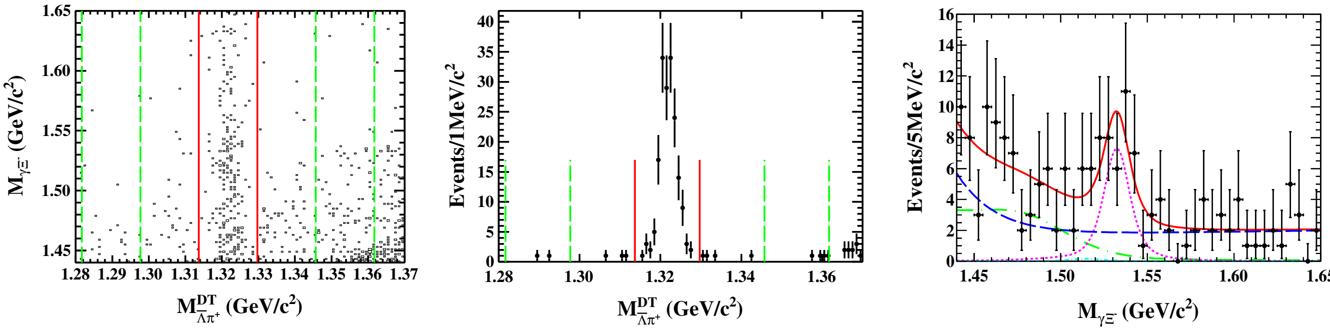

FIG. 2. Left: scatter plot of $M_{\gamma\Xi^-}$ versus $M^{\rm DT}_{\bar{\Lambda}\pi^+}$ from the data, where $M^{\rm DT}_{\bar{\Lambda}\pi^+}$ is the $\bar{\Lambda}\pi^+$ invariant mass spectrum in the DT mode. Middle: the $M^{\rm DT}_{\bar{\Lambda}\pi^+}$ distribution from the data. The red solid and green long-dashed lines indicate the $\bar{\Xi}^+$ signal and sideband regions, respectively. Right: the fit to the experimental $M_{\gamma\Xi^-}$ distribution. The red solid line is the fit result, the pink dotted line denotes the signal component, the cyan dash-dotted line describes the few peaking background events from the process $J/\psi \to \Xi(1530)^-\bar{\Xi}^+$ with $\Xi(1530)^-$ decaying to the $\Xi^-\pi^0$ and $\Xi^0\pi^-$ systems, the green long-dash-dotted line denotes the background events from $J/\psi \to \gamma\eta_c \to \gamma\Xi^-\bar{\Xi}^+$, and the blue long-dashed line denotes the contribution from the remaining background events.

from the inclusive MC sample in which the main background processes (see below in the section) are known and normalized using PDG branching fraction values [9]. Three iterations between the S value and the χ^2_{4C} requirement are employed until the procedure is converged.

The $\gamma\Xi^-$ invariant mass spectrum of the events that remain after imposing the selection criteria above are shown in Fig. 2 (right). A weak enhancement of events in the region of the radiative $\Xi(1530)^-$ decay can be seen.

The background sources are divided into two categories, one with and one without the Ξ^- resonance. The non-Ξ^- backgrounds are investigated by the Ξ^- mass sideband events, where the sideband regions are defined as in the ST mode (see Sec. III A). It is found that very few events from the sidebands survived in the $M_{\gamma\Xi^-}$ region around 1.535 GeV$/c^2$. According to the inclusive MC information, the main background is the decay $J/\psi \to \gamma\eta_c \to \gamma\Xi^-\bar{\Xi}^+$, which distributes smoothly in the signal region of the $\Xi(1530)^-$ baryon. Only a few peaking background events contributing to the $\Xi(1530)$ mass region are found from the process $J/\psi \to \Xi(1530)^-\bar{\Xi}^+$ with $\Xi(1530)^-$ decaying to the $\Xi^-\pi^0$ and $\Xi^0(\to \Lambda\pi^0)\pi^-$ systems with a soft photon being undetected. Other background events, forming a flat distribution in the $\gamma\Xi^-$ mass spectrum, arise from the decays $J/\psi \to \gamma\Xi^-\bar{\Xi}^+$ and $J/\psi \to \Xi^-\bar{\Xi}^+$.

The signal yields for the decay $J/\psi \to \Xi(1530)^-\bar{\Xi}^+ \to \gamma\Xi^-\bar{\Xi}^+$ are extracted by an unbinned maximum likelihood fit to the $M_{\gamma\Xi^-}$ spectrum. The shape of the invariant mass distribution of the $\Xi(1530)^-$ baryon is modeled based on the prediction of the simulation. The few peaking background events from the process $J/\psi \to \Xi(1530)^-\bar{\Xi}^+$, with $\Xi(1530)^-$ decaying to the $\Xi^-\pi^0$ and $\Xi^0(\to \Lambda\pi^0)\pi^-$ systems, are normalized with their branching fractions, where $\mathcal{B}(J/\psi \to \Xi(1530)^-\bar{\Xi}^+)$ is obtained from this work and the branching fractions of two $\Xi(1530)^-$ decays are from the PDG [9]. The smooth and dominating background from $J/\psi \to \gamma\eta_c \to \gamma\Xi^-\bar{\Xi}^+$ events is described by the MC-determined shape, where the corresponding number [9] of the background events is normalized to the data. The remaining background shape is parametrized by an exponential function plus a first-order polynomial to describe the inclined flat slope in the $M_{\gamma\Xi^-}$ distribution from the two main backgrounds, $J/\psi \to \gamma\Xi^-\bar{\Xi}^+$ and $J/\psi \to \Xi^-\bar{\Xi}^+$. The parameters of the exponential function and the first-order polynomial are fitted. The fit, shown in Fig. 2 (right), yields 33.2 ± 9.6 signal events with a significance of 3.9σ which is the most conservative one among various fit scenarios (i.e., different fit range, signal shape, background shape, and background size). The significance is calculated from the test-statistic $\sqrt{-2\ln(\mathcal{L}_0/\mathcal{L}_{\rm max})}$ assuming Wilk's theorem [33], where $\mathcal{L}_{\rm max}$ and $\mathcal{L}_0$ are the likelihoods of the fits with and without the $\Xi(1530)^-$ signal included, respectively. The upper limit on the signal yield is determined by convolving the likelihood distribution with a Gaussian function with a standard deviation of $\sigma = x \times \Delta$, where

TABLE II. Systematic uncertainties on the branching fraction measurements. Here, Ξ^{*-} denotes the $\Xi(1530)^-$ resonance.

Source	$J/\psi \to \Xi^{*-}\bar{\Xi}^+(\%)$	$\Xi^{*-} \to \gamma\Xi^-(\%)$
Photon	⋯	1.0
$\bar{\Xi}^+$ efficiency correction	0.7	0.7
$\bar{\Lambda}/\Lambda$ mass window	0.2	0.2
$\bar{\Xi}^+/\Xi^-$ mass window	1.4	1.4
$\bar{\Lambda}/\Lambda$ decay length	0.1	0.1
$\bar{\Xi}^+/\Xi^-$ decay length	1.0	1.0
Kinematic fit	⋯	2.4
Angular distribution	0.5	3.6
Fit procedure	1.2	⋯
Intermediate decays	0.8	0.8
$N_{J/\psi}$	0.5	⋯
In total	2.5	4.9

x is the number of fitted signal events, and Δ refers to the total systematic uncertainty (4.9%, see Table II). It is found to be $N_{\rm DT}^{\rm UL} = 46$ at the 90% C.L.

IV. MEASUREMENTS OF BRANCHING FRACTIONS AND ANGULAR DISTRIBUTION

A. Measurements of $\mathcal{B}(J/\psi \to \Xi(1530)^- \bar{\Xi}^+)$ and $\mathcal{B}(\Xi(1530)^- \to \gamma\Xi^-)$

The branching fraction for $J/\psi \to \Xi(1530)^- \bar{\Xi}^+$ is calculated using

$$\mathcal{B}(J/\psi \to \Xi(1530)^- \bar{\Xi}^+) = \frac{N_{\rm ST}^{\rm obs}}{N_{J/\psi}\mathcal{B}(\bar{\Xi}^+)\mathcal{B}(\bar{\Lambda})\epsilon_{\rm ST}}, \quad (2)$$

where $N_{\rm ST}^{\rm obs}$ is the number of events for ST, which is extracted from the fit to $M_{\bar{\Lambda}\pi^+}^{\rm recoil}$ spectrum; $N_{J/\psi}$ is the total number of J/ψ events [12]; $\mathcal{B}(\bar{\Xi}^+)$ and $\mathcal{B}(\bar{\Lambda})$ are the branching fractions [9] of $\bar{\Xi}^+ \to \bar{\Lambda}\pi^+$ and $\bar{\Lambda} \to \bar{p}\pi^+$, respectively; $\epsilon_{\rm ST}$, expressed as $(f^+\epsilon_{\rm ST}^{\bar{\Xi}^+} + f^-\epsilon_{\rm ST}^{\Xi^-})/2$, is the average detection efficiency in the ST mode for both the charge-conjugate processes, where $\epsilon_{\rm ST}^{\bar{\Xi}^+}(\epsilon_{\rm ST}^{\Xi^-})$ denotes the MC-simulated efficiency for only tagging $\bar{\Xi}^+(\Xi^-)$ decay mode, and $f^+(f^-)$ is the correction factor for the $\bar{\Xi}^+$ (Ξ^-) reconstruction efficiency estimated by using a control sample of $J/\psi \to \Xi^-\bar{\Xi}^+$ with all polarization parameters considered. Here, $f^+(f^-)$ is the ratio of the $\bar{\Xi}^+$ (Ξ^-) reconstruction efficiency in the data $[\epsilon_{\rm data}^{\bar{\Xi}^+}$ $(\epsilon_{\rm data}^{\Xi^-})]$ to that in the MC sample $[\epsilon_{\rm MC}^{\bar{\Xi}^+}$ $(\epsilon_{\rm MC}^{\Xi^-})]$, i.e., $f^+ = \epsilon_{\rm data}^{\bar{\Xi}^+}/\epsilon_{\rm MC}^{\bar{\Xi}^+}$ $(f^- = \epsilon_{\rm data}^{\Xi^-}/\epsilon_{\rm MC}^{\Xi^-})$. As a result, the branching fraction of $\mathcal{B}(J/\psi \to \Xi(1530)^- \bar{\Xi}^+)$ is determined to be $(3.17 \pm 0.02) \times 10^{-4}$ where the uncertainty is statistical only, and other numerical values are listed in Table I.

The upper limit at the 90% C.L. on the branching fraction for the radiative decay $\Xi(1530)^- \to \gamma\Xi^-$ is calculated using

$$\mathcal{B}^{\rm UL}(\Xi(1530)^- \to \gamma\Xi^-) = \frac{N_{\rm DT}^{\rm UL}}{N_{J/\psi}\mathcal{B}(J/\psi \to \Xi(1530)^-\bar{\Xi}^+)\mathcal{B}(\bar{\Xi}^+)\mathcal{B}(\bar{\Lambda})\mathcal{B}(\Xi^-)\mathcal{B}(\Lambda)\epsilon_{\rm DT}} = \frac{N_{\rm DT}^{\rm UL}\epsilon_{\rm ST}}{\mathcal{B}(\Xi^-)\mathcal{B}(\Lambda)N_{\rm ST}^{\rm obs}\epsilon_{\rm DT}}, \quad (3)$$

where $N_{\rm DT}^{\rm UL}$ is the upper limit on the number of fitted $\Xi(1530)^- \to \gamma\Xi^-$ signal events at the 90% C.L.; $\mathcal{B}(\Xi^-)$ and $\mathcal{B}(\Lambda)$ are the branching fractions [9] of $\Xi^- \to \Lambda\pi^-$ and $\Lambda \to p\pi^-$, respectively; $\epsilon_{\rm DT}$, expressed as $f^-f^+\epsilon_{\rm DT}^{\rm MC}$, is the detection efficiency in the DT mode, where $\epsilon_{\rm DT}^{\rm MC}$ denotes the MC-simulated efficiency using the J2BB3 model [28]. Taking the systematic uncertainty (see Sec. V A) into consideration, the upper limit at the 90% C.L. on the branching fraction of $\Xi(1530)^- \to \gamma\Xi^-$ is calculated to be 3.7%.

B. Measurement of the angular distribution in $J/\psi \to \Xi(1530)^- \bar{\Xi}^+$

We obtain the number of recorded $J/\psi \to \Xi(1530)^- \bar{\Xi}^+$ events in each cosθ bin by fitting the $\bar{\Lambda}\pi^+$ invariant mass distribution as described in Sec. IV A. By dividing by the detection efficiency in each cosθ interval, we obtain the efficiency-corrected cosθ distribution shown in Fig. 3. A least square fit of Eq. (1) to the obtained cosθ distribution in the range of $[-1.0, 1.0]$ gives $\alpha = -0.20 \pm 0.04$, where the uncertainty is statistical only.

V. SYSTEMATIC UNCERTAINTIES

A. Branching fractions

The systematic uncertainties in the branching fraction measurements arise from many sources. They depend on the $\bar{\Xi}^+$ efficiency correction, mass windows for $\bar{\Lambda}$ and $\bar{\Xi}^+$, decay lengths for $\bar{\Lambda}$ and $\bar{\Xi}^+$, background shape, the amount of background, the branching fractions of the intermediate decays, and the total number of J/ψ events. It is noteworthy that the uncertainties due to the tracking and particle identification efficiencies for the charged π track from the $\bar{\Xi}^+$ decay and the $\bar{\Lambda}$ reconstruction efficiency are included in the charged $\bar{\Xi}^+$ reconstruction uncertainty. For the radiative $\Xi(1530)^-$ decay they depend, in addition, on the photon reconstruction efficiency.

(1) Photon reconstruction efficiency: The uncertainty on the photon detection efficiency is 1.0% per photon,

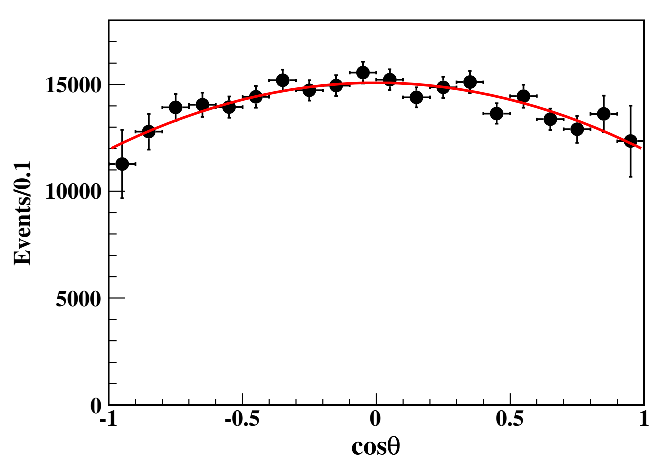

FIG. 3. The cosθ distribution for $J/\psi \to \Xi(1530)^- \bar{\Xi}^+$. The dots with error bars denote the efficiency-corrected data, and the red curve is the fit result.

obtained by studying $J/\psi \to \rho^0\pi^0$, $\rho^0 \to \pi^+\pi^-$, $\pi^0 \to \gamma\gamma$ events [34].

(2) $\bar{\Xi}^+$ efficiency correction: As mentioned above, the correction factor $f^+(f^-)$ on the $\bar{\Xi}^+$ (Ξ^-) reconstruction efficiency, defined as $\epsilon^{\bar{\Xi}^+}_{\rm data}/\epsilon^{\bar{\Xi}^+}_{\rm MC}$ ($\epsilon^{\Xi^-}_{\rm data}/\epsilon^{\Xi^-}_{\rm MC}$), is obtained by using a control sample of $J/\psi \to \bar{\Xi}^+\Xi^-$ decays via single and double tag methods (the values are listed in Table I). The uncertainty on $f^+(f^-)$, obtained by adding the relative uncertainties for $\epsilon^{\bar{\Xi}^+}_{\rm data}$ and $\epsilon^{\bar{\Xi}^+}_{\rm MC}$ ($\epsilon^{\Xi^-}_{\rm data}$ and $\epsilon^{\Xi^-}_{\rm MC}$) in quadrature assuming the sources are independent, is found to be 1.0% for each mode. Therefore, the systematic uncertainty for $\bar{\Xi}^+$ efficiency correction is taken as 0.7% by averaging both charge-conjugate modes.

(3) Mass window (decay length) of $\bar{\Lambda}$ ($\bar{\Xi}^+$): The uncertainty attributed to the $\bar{\Lambda}$ ($\bar{\Xi}^+$) mass window (decay length) requirement is estimated using $|\varepsilon_{\rm data} - \varepsilon_{\rm MC}|/\varepsilon_{\rm data}$, where $\varepsilon_{\rm data}$ is the efficiency of applying the $\bar{\Lambda}$ ($\bar{\Xi}^+$) mass window (decay length) requirement by extracting $\bar{\Lambda}$ ($\bar{\Xi}^+$) signal in the $\bar{p}\pi^+$ ($\bar{\Lambda}\pi^+$) invariant mass spectrum of the data, and $\varepsilon_{\rm MC}$ is the corresponding efficiency from the MC simulation. The difference between the data and the MC simulation is considered as the systematic uncertainty and is found to be 0.2% (0.1%) due to the $\bar{\Lambda}$ mass window (decay length) requirement, and 1.4% (1.0%) for the $\bar{\Xi}^+$ mass window (decay length) requirement.

(4) Kinematic fit for the radiative $\Xi(1530)^-$ decay mode: Correcting the tracking helix parameters [35] reduces the difference between MC simulation and data. The uncertainty of 2.4% due to the kinematic fit is estimated by the observed differences between an analysis that accounts for such correction and an analysis that does not. The correction factors obtained by control sample $J/\psi \to p\bar{p}\pi^+\pi^-$ and gives 2.4% as the estimated systematic uncertainty.

(5) Angular distribution: The systematic uncertainty of angular distribution is estimated to take the larger difference of the detection efficiency by varying the measured α values by $\pm 1\sigma$ in the MC simulation. And it is determined to be 0.5% and 3.6% for the inclusive and radiative $\Xi(1530)^-$ decay modes, respectively.

(6) Fit procedure: For the inclusive $\Xi(1530)^-$ decay mode, uncertainties due to the fitting range of $M^{\rm recoil}_{\bar{\Lambda}\pi^+}$ are estimated by changing the fitting range from 1.47–1.62 GeV/c^2 to 1.475–1.615 GeV/c^2 and 1.465–1.625 GeV/c^2, respectively. The largest difference with respect to the nominal value is 0.7%, and this is taken as the uncertainty associated with the fitting range. The uncertainty due to the background shape is estimated by changing the second-order polynomial function to a first-order polynomial. The relative difference on the signal yield of 1.0% is taken as the uncertainty due to the background shape. In the fit of $M^{\rm recoil}_{\bar{\Lambda}\pi^+}$, the signal shape is parametrized by the simulated MC shape convolved with a Gaussian function with the mean of zero. To estimate the uncertainty caused by a possible shift of the signal peak, an alternative model with the free mean of the Gaussian is used to estimate the uncertainty due to the signal shape. The difference between the two fits of 0.02% is negligible. Assuming that the sources above are independent and adding them in quadrature, the total systematic uncertainty associated with the fit procedure is obtained to be 1.2%. As for the radiative $\Xi(1530)^-$ decay mode, the uncertainty associated with the fit procedure is negligible since the nominal upper limit on $\mathcal{B}(\Xi(1530)^- \to \gamma\Xi^-)$ is the most conservative one among multiple fit scenarios.

(8) Intermediate decays: The uncertainties due to the branching fractions of intermediate decays $\Xi^- \to \Lambda\pi^-$ and $\Lambda \to p\pi^-$ are 0.04% and 0.8% [9], respectively. Therefore, this uncertainty associated with the branching fractions of intermediate decays is taken to be 0.8%.

(9) Number of J/ψ events: The total number of J/ψ events is obtained by studying the inclusive hadronic J/ψ decays which has a systematic uncertainty of 0.5% [12].

Table II lists all systematic uncertainties on branching fraction measurements for the $J/\psi \to \Xi(1530)^-\bar{\Xi}^+$ decay in the ST mode and the radiative $\Xi(1530)^-$ decay mode, respectively. The total systematic uncertainty is individually calculated as the quadratic sum of all individual terms for each mode.

B. Angular distribution

The systematic uncertainties in the measurement of the α value arise from $M^{\rm recoil}_{\bar{\Lambda}\pi^+}$ fitting range, background shape, $\cos\theta$ fitting range, $\cos\theta$ binning, and efficiency correction. It should be noted that the absolute value of the difference between the remeasured α values in the alternative cases mentioned above and the nominal value is taken as the uncertainty given in this analysis.

(1) The $M^{\rm recoil}_{\bar{\Lambda}\pi^+}$ fitting range: The uncertainty due to the fitting range of $M^{\rm recoil}_{\bar{\Lambda}\pi^+}$ is estimated by changing the fitting range from 1.47–1.62 GeV/c^2 to 1.475–1.615 GeV/c^2 and 1.465–1.625 GeV/c^2, respectively. The largest difference for $\alpha_{\Xi(1530)^-}$ of 0.02 is taken as the uncertainty due to the fitting range.

(2) The background shape: The uncertainty due to the background shape in the angular distribution is estimated by changing the second-order polynomial function applied for fitting $M^{\rm recoil}_{\bar{\Lambda}\pi^+}$ to a first-order polynomial function. The difference becomes 0.04 for $\alpha_{\Xi(1530)^-}$, and this is taken as the uncertainty due to the background shape.

TABLE III. Absolute systematic uncertainties on the α value.

Source	$\alpha_{\Xi(1530)^-}$
$M^{\rm recoil}_{\bar{\Lambda}\pi^+}$ fitting range	0.02
Background shape	0.04
$\cos\theta$ fitting range	0.01
$\cos\theta$ binning	0.01
Efficiency correction	0.03
Total uncertainty	0.06

(3) The cosθ fitting range: The uncertainty due to the cosθ fitting range is estimated by varying the $\cos\theta$ fitting range to [−0.9, 0.9]. The difference on angular distribution is 0.01, and this is taken as the uncertainty due to the cosθ fitting range.

(4) The $\cos\theta$ binning: The uncertainty due to the binning of $\cos\theta$ is estimated by changing the nominal choice of 20 bins to 10 bins. The difference for α value between the two cases of 0.01 is taken as the systematic uncertainty due to the binning.

(5) Efficiency correction: The α value is obtained by fitting the efficiency-corrected $\cos\theta$ distribution. To estimate the systematic uncertainty due to the MC generator to the fitted α value, the ratio of detection efficiencies between the data and MC simulation is obtained based on the process $J/\psi \to \Xi(1530)^-\bar{\Xi}^+$ with the inclusive decay of $\Xi(1530)^-$. The $\cos\theta$ distribution is refitted using corrected one by the above ratio of detection efficiencies. The resulting absolute difference of 0.03 in α is taken as the systematic uncertainty due to the imperfection of MC simulation.

The absolute systematic uncertainties from the different sources for the α parameter of the angular distribution are given in Table III, and the total systematic uncertainty is obtained by adding the values in quadrature, assuming that the sources of uncertainty are independent.

VI. SUMMARY AND DISCUSSION

The SU(3)-flavor violating decay $J/\psi \to \Xi(1530)^-\bar{\Xi}^+$ is measured using $(1310.6 \pm 7.0) \times 10^6$ J/ψ events collected with the BESIII detector in 2009 and 2012. The signal is clearly observed ($> 10\sigma$), and the branching fraction is measured to be $\mathcal{B}(J/\psi \to \Xi(1530)^-\bar{\Xi}^+ + \text{c.c.}) = (3.17 \pm 0.02 \pm 0.08) \times 10^{-4}$. The result is consistent with the DM2 measurement [7] within 2 standard deviations (see Table IV), but with an order of magnitude improved precision. The α value of the angular distribution for $J/\psi \to \Xi(1530)^-\bar{\Xi}^+$ decay is measured for the first time and is found to be $\alpha_{\Xi(1530)} = -0.21 \pm 0.04 \pm 0.06$.

In addition, we present the first evidence for the $\Xi(1530)^- \to \gamma\Xi^-$ radiative decay with a significance of 3.9σ. The upper limit at the 90% C.L. on the branching fraction of $\Xi(1530)^- \to \gamma\Xi^-$ is measured to be 3.7%, which is consistent with the previous measurement [23]. The result is compatible with the theoretical prediction of 3.0×10^{-4} [3,20]. Our result provides complementary experimental information for isolating both the octet-decuplet mixing mechanism [20] and meson cloud effects [3] in the baryon structure.

ACKNOWLEDGMENTS

The BESIII Collaboration thanks the staff of BEPCII and the IHEP computing center for their strong support. This work is supported in part by National Key Basic Research Program of China under Contract No. 2015CB856700; National Natural Science Foundation of China (NSFC) under Contracts No. 11565006, No. 11605042, No. 11625523, No. 11635010, No. 11735014, No. 11835012, No. 11935018; the Chinese Academy of Sciences (CAS) Large-Scale Scientific Facility Program; Joint Large-Scale Scientific Facility Funds of the NSFC and CAS under Contracts No. U1232107, No. U1532257, No. U1532258, No. U1732263, No. U1832207; CAS Key Research Program of Frontier Sciences under Contracts No. QYZDJ-SSW-SLH003, No. QYZDJ-SSW-SLH040; 100 Talents Program of CAS; INPAC and Shanghai Key Laboratory for Particle Physics and Cosmology; German Research Foundation DFG under Contract No. Collaborative Research Center CRC 1044; Istituto Nazionale di Fisica Nucleare, Italy; Koninklijke Nederlandse Akademie van Wetenschappen (KNAW) under Contract No. 530-4CDP03; Ministry of Development of Turkey under Contract No. DPT2006K-120470; National Science and Technology fund; The Knut and Alice Wallenberg Foundation (Sweden) under Contract No. 2016.0157; The Swedish Research Council; U.S. Department of Energy under Contracts No. DE-FG02-05ER41374, No. DE-SC-0010118, No. DE-SC-0012069; University of Groningen (RuG) and the Helmholtzzentrum fuer Schwerionenforschung GmbH (GSI), Darmstadt; China

TABLE IV. Comparison of the results from this measurements to previous work.

	This work	Other measurements	Theoretical prediction
$\mathcal{B}(J/\psi \to \Xi(1530)^-\bar{\Xi}^+ + \text{c.c.})$ (10^{-4})	$3.17 \pm 0.02 \pm 0.08$	$5.9 \pm 0.9 \pm 1.2$ [7]	...
$\alpha(J/\psi \to \Xi(1530)^-\bar{\Xi}^+)$	$-0.21 \pm 0.04 \pm 0.06$	...	...
$\mathcal{B}(\Xi(1530)^- \to \gamma\Xi^-)(\%)$	≤ 3.7 @ 90% C.L.	≤ 4 @ 90% C.L. [23]	~0.03 [3,20]

Postdoctoral Science Foundation under Contract No. 2017M622347, Postdoctoral research start-up fees of Henan Province under Contract No. 2017SBH005, Ph.D research start-up fees of Henan Normal University under Contract No. qd16164, Program for Innovative Research Team in University of Henan Province (Grant No. 19IRTSTHN018).

[1] D. M. Asner *et al.*, Int. J. Mod. Phys. A **24**, 247 (2009).
[2] L. Köpke and N. Wermes, Phys. Rep. **174**, 67 (1989).
[3] G. Ramalho and K. Tsushima, Phys. Rev. D **87**, 093011 (2013).
[4] Inclusion of charge-conjugate decay mode is implicit unless otherwise stated.
[5] H. Kowalski and T. F. Walsh, Phys. Rev. D **14**, 852 (1976).
[6] Unless otherwise indicated in the paper, a single number on the uncertainty refers to the sum in quadrature of the statistical item and the systematic one; if there are two uncertainties, the first one is statistical, and the second systematic.
[7] P. Henrard *et al.* (DM2 Collaboration), Nucl. Phys. **B292**, 670 (1987).
[8] M. Ablikim *et al.* (BESIII Collaboration), Phys. Rev. D **100**, 051101(R) (2019).
[9] M. Tanabashi *et al.* (Particle Data Group), Phys. Rev. D **98**, 030001 (2018).
[10] A. Zhang, Y. R. Liu, P. Z. Huang, W. Z. Deng, X. L. Chen, and S. L. Zhu, Chin. Phys. C **29**, 250 (2005), http://cpc.ihep.ac.cn/article/id/dfda0110-74a4-4b0b-a5c8-a75b86ca9b36.
[11] M. Ablikim *et al.* (BESIII Collaboration), Chin. Phys. C **36**, 915 (2012).
[12] M. Ablikim *et al.* (BESIII Collaboration), Chin. Phys. C **41**, 013001 (2017).
[13] S. J. Brodsky and G. P. Lepage, Phys. Rev. D **24**, 2848 (1981).
[14] M. Claudson, S. L. Glashow, and M. B. Wise, Phys. Rev. D **25**, 1345 (1982).
[15] C. Carimalo, Int. J. Mod. Phys. A **02**, 249 (1987).
[16] F. Murgia and M. Melis, Phys. Rev. D **51**, 3487 (1995).
[17] H. Chen and R. G. Ping, Phys. Lett. B **644**, 54 (2007).
[18] M. Ablikim *et al.* (BES Collaboration), Phys. Lett. B **632**, 181 (2006).
[19] M. Ablikim *et al.* (BESIII Collaboration), Phys. Rev. D **93**, 072003 (2016); Phys. Lett. B **770**, 217 (2017).
[20] E. Kaxiras, E. J. Moniz, and M. Soyeur, Phys. Rev. D **32**, 695 (1985).
[21] F. Myhrer, Phys. Rev. C **74**, 065202 (2006).
[22] H. B. Li, Front. Phys. **12**, 121301 (2017); **14**, 64001(E) (2019).
[23] G. R. Kalbfleisch, R. C. Strand, and J. W. Chapman, Phys. Rev. D **11**, 987 (1975).
[24] M. Ablikim *et al.* (BESIII Collaboration), Nucl. Instrum. Methods Phys. Res., Sect. A **614**, 345 (2010).
[25] Z. Y. Deng, G. F. Cao, and C. D. Fu *et al.*, Chin. Phys. C **30**, 371 (2006), http://cpc.ihep.ac.cn/article/id/283d17c0-e8fa-4ad7-bfe3-92095466def1.
[26] S. Agostinelli *et al.* (GEANT4 Collaboration), Nucl. Instrum. Methods Phys. Res., Sect. A **506**, 250 (2003).
[27] J. Allison *et al.*, IEEE Trans. Nucl. Sci. **53**, 270 (2006).
[28] R. G. Ping and C. Y. Pang, Monte Carlo generators for Tau-Charm-Physics at BESIII, http://bes.ihep.ac.cn/bes3/phy_book/book/phy/generators_ping.pdf.pdf.
[29] S. Jadach, B. F. L. Ward, and Z. Was, Comput. Phys. Commun. **130**, 260 (2000); Phys. Rev. D **63**, 113009 (2001).
[30] D. Lange, Nucl. Instrum. Methods Phys. Res., Sect. A **462**, 152 (2001); R. G. Ping, Chin. Phys. C **32**, 599 (2008).
[31] J. C. Chen, G. S. Huang, X. R. Qi, D. H. Zhang, and Y. S. Zhu, Phys. Rev. D **62**, 034003 (2000).
[32] M. Xu *et al.*, Chin. Phys. C **33**, 428 (2009).
[33] S. I. Bityukov and N. V. Krasnikov, Nucl. Instrum. Methods Phys. Res., Sect. A **452**, 518 (2000).
[34] M. Ablikim *et al.* (BESIII Collaboration), Phys. Rev. D **83**, 112005 (2011).
[35] M. Ablikim *et al.* (BESIII Collaboration), Phys. Rev. D **87**, 012002 (2013).